

Electrical isolation of ZnO by ion bombardment

S. O. Kucheyev,^{a)} P. N. K. Deenapanray, C. Jagadish, and J. S. Williams

Department of Electronic Materials Engineering, Research School of Physical Sciences and Engineering, The Australian National University, Canberra, ACT 0200, Australia

Mitsuaki Yano, Kazuto Koike, Shigehiko Sasa, and Masataka Inoue

New Materials Research Center and Bio-Venture Center, Osaka Institute of Technology, Asahi-ku, Ohmiya, Osaka 535-8585, Japan

Ken-ichi Ogata

Bio-Venture Center, Osaka Institute of Technology, Asahi-ku, Ohmiya, Osaka 535-8585, Japan

(Received 20 May 2002; accepted 9 September 2002)

The evolution of sheet resistance of *n*-type single-crystal wurtzite ZnO epilayers exposed to bombardment with MeV ¹H, ⁷Li, ¹⁶O, and ²⁸Si ions at room temperature is studied *in situ*. We demonstrate that sheet resistance of ZnO can be increased by about 7 orders of magnitude as a result of ion irradiation. Due to extremely efficient dynamic annealing in ZnO, the ion doses needed for isolation of this material are about 2 orders of magnitude larger than corresponding doses in the case of another wide-bandgap semiconductor, GaN. Results also show that the ion doses necessary for electrical isolation close-to-inversely depend on the number of ion-beam-generated atomic displacements. However, in all the cases studied, defect-induced electrical isolation of ZnO is unstable to rapid thermal annealing at temperatures above ~300 °C. © 2002 American Institute of Physics. [DOI: 10.1063/1.1518560]

Recently, research on ZnO has received significant interest due to important potential applications of this material in the fabrication of short-wavelength optoelectronic devices as well as devices for high-temperature/high-power electronics.¹ Practical advantages of ZnO over another wide-band-gap semiconductor—GaN, which currently dominates the market of short-wavelength optoelectronics—include a bulk growth capability, amenability to conventional chemical wet etching, and convenient cleavage planes.¹ Further main advantages of ZnO as a light emitter are (i) a direct band gap which can be tuned from 2.8 to 4 eV by alloying ZnO with CdO and MgO, (ii) a large excitonic binding energy (60 meV), which will be useful for UV laser applications, and (iii) low power thresholds for optical pumping at room temperature (RT). For electronic applications, additional attractiveness of ZnO lies in having a high breakdown strength and a high saturation velocity.¹

Such excellent fundamental material properties as well as recent significant success in the growth of high-quality single crystals make ZnO an ideal candidate for (opto)electronic device applications.¹ However, in addition to desired fundamental properties, the fabrication of ZnO-based (opto)electronic devices obviously requires development of a device processing technology. Indeed, at present, there are significant challenges for processing ZnO including electrical doping, metallization, and electrical isolation. Ion implantation, an attractive device processing tool, can be used for selective-area doping and electrical isolation. In the latter case, ion irradiation can render the material highly resistive under appropriate conditions.² It is generally believed that irradiation-induced degradation of carrier mobility as well as

the trapping of carriers at deep centers associated with irradiation-produced damage (defect isolation) or with implanted species (chemical isolation) is the mechanism responsible for electrical isolation of semiconductors.²

Although electrical properties of single-crystal ZnO bombarded with electrons or light ions have previously been studied,³⁻⁷ we are not aware of any reports demonstrating that ZnO can be rendered highly resistive, as required for electrical isolation. In this letter, we demonstrate irradiation-induced formation of highly resistive layers in *n*-type single-crystal ZnO epilayers grown on sapphire substrates. For isolation, we have used MeV light ions whose projected ranges are considerably greater than the thickness of the ZnO epilayers studied. In this case, the profiles of ion-generated atomic displacements are essentially uniform throughout the conductive ZnO film. A single MeV implant, hence, is sufficient to isolate a relatively thick ZnO film. Moreover, irradiation with MeV ions has allowed us to separate the effects of defect isolation from chemical isolation and to avoid the formation of a layer with substantial defect-induced (hopping) conduction, which inevitably forms at the ion end-of-range region in the case of keV implants and usually complicates the interpretation of data.² We have also investigated thermal stability of electrical isolation in ZnO.

The *n*-type single-crystal wurtzite ZnO epilayers used in this study were ~0.6 μm thick, epitaxially grown on *a*-plane sapphire substrates by molecular beam epitaxy at OIT. A further description of growth conditions can be found elsewhere.⁸ As-grown epilayers had a RT free electron concentration of ~10¹⁷ cm⁻³, an effective Hall mobility of ~80 cm² V⁻¹ s⁻¹, and a sheet resistance of ~1 kΩ/sq. Resistors of ~3.5×3.5 mm² in size were prepared with InGa eutectic ohmic contacts on two opposite sides of each sample.

^{a)}Present address: Lawrence Livermore National Laboratory, Livermore, CA 94550; electronic mail: kucheyev1@llnl.gov

TABLE I. Implant conditions used in this study. Calculated values of projected ion ranges (R_p) and the average number of lattice vacancies produced by one ion (N_{vac}) within the 0.6- μm -thick ZnO epilayer are also given.

Ion	Energy (MeV)	Doses (10^{12} cm^{-2})	Beam flux ($10^{11} \text{ cm}^{-2} \text{ s}^{-1}$)	Implantation temperature ($^{\circ}\text{C}$)	R_p (μm)	N_{vac}
^1H	0.6	1.0–78000	0.04–2	20	4.58	0.3
^7Li	0.7	0.5–1200	1.9	20	1.63	19.5
^{16}O	2.0	0.5–1000	1.9	20	1.87	105.1
^{28}Si	3.5	0.3–1000	1.0	20	1.79	251.0

These ZnO resistors were bombarded in an ANU 1.7 MV tandem accelerator (NEC, 5SDH-4) under ion irradiation conditions given in Table I. Ion energies were chosen to place the damage peak deep into the sapphire substrate, beyond the ZnO layer, as clearly seen from a comparison of projected ion ranges (calculated with the TRIM code⁹) also given in Table I. During ion bombardment, samples were tilted by $\sim 7^{\circ}$ off the surface normal direction to minimize channeling. Sheet resistance (R_s) was measured *in situ* after each dose step using a Keithley 619 electrometer. Postirradiation isochronal annealing was carried out in a rapid thermal annealing (RTA) system for 60 s at temperatures from 100 up to 1000 $^{\circ}\text{C}$ in an Ar ambient at atmospheric pressure.

Figure 1(a) shows the evolution of R_s of ZnO resistors irradiated with 0.6 MeV H, 0.7 MeV Li, 2 MeV O, and 3.5 MeV Si ions at RT. It is seen from Fig. 1(a) that, similar to

the situation for other semiconductors,^{2,10,11} the ion dose dependence of R_s , for each particular ion, has three distinct regions: (i) a low dose region where R_s increases only slightly with increasing ion dose, (ii) a relatively narrow intermediate dose region characterized by a very rapid increase in R_s (by ~ 7 orders of magnitude), and (iii) the third region for large doses where R_s reaches its maximum value, remaining approximately constant with further increasing ion dose. In all the samples studied (except for the case of H ion irradiation when even larger ion doses are needed for complete isolation), the values of R_s reach the maximum after some characteristic dose (the so called threshold isolation dose,^{10,11} Φ_{th}). The levels of R_s at the plateaus shown in Fig. 1(a) for doses above Φ_{th} are $\sim 4 \times 10^{10} \Omega/\text{sq}$. However, it should be noted that the real maximum values of R_s can be even larger because the R_s values measured have a contribution from the parasitic resistances of the experimental setup, which are of the same order of magnitude.

Figure 1(a) also shows that the isolation curves progressively shift toward lower doses with increasing ion mass. Such a shift is caused by an increase in the number of ion-beam-generated atomic displacements with increasing ion mass, as can be seen from the last column of Table I calculated with the TRIM code⁹ with a threshold displacement energy of 57 eV for both Zn and O sublattices, based on data from Ref. 3. This ion mass effect is better illustrated in Fig. 1(b), showing the average number of lattice vacancies produced by different ions within ZnO epilayers (see Table I) versus both Φ_{th} and doses required to produce a R_s of 0.1 M Ω/sq [indicated as $\Phi(0.1 \text{ M}\Omega/\text{sq})$]. Straight line fits with slopes of -1.14 ± 0.10 and -1.02 ± 0.02 represent the best fits to Φ_{th} and $\Phi(0.1 \text{ M}\Omega/\text{sq})$ dependencies, respectively. Thus, results from Fig. 1(b) indicate that the efficiency of the carrier removal process close-to-inversely depends on the number of ion-beam-generated atomic displacements.¹²

It is interesting to make a comparison of results of the present study with isolation data for another wide-bandgap semiconductor, GaN, studied in detail previously (see, for example, Refs. 10 and 11). First of all, a comparison of Fig. 1 with previous isolation data^{10,11} shows that the ion doses (and, hence, the number of ion-beam-generated atomic displacements) needed to isolate ZnO are ~ 2 orders of magnitude larger than isolation doses in the case of GaN. This is a direct consequence of extremely efficient dynamic annealing of ion-beam-generated point defects in ZnO (i.e., migration and interaction of defects *during* ion irradiation), as studied in a number of previous reports.^{3,5–7,13–15} Due to a large mobility of Frenkel pairs in ZnO, most of ion-beam-generated point defects experience annihilation, and only a

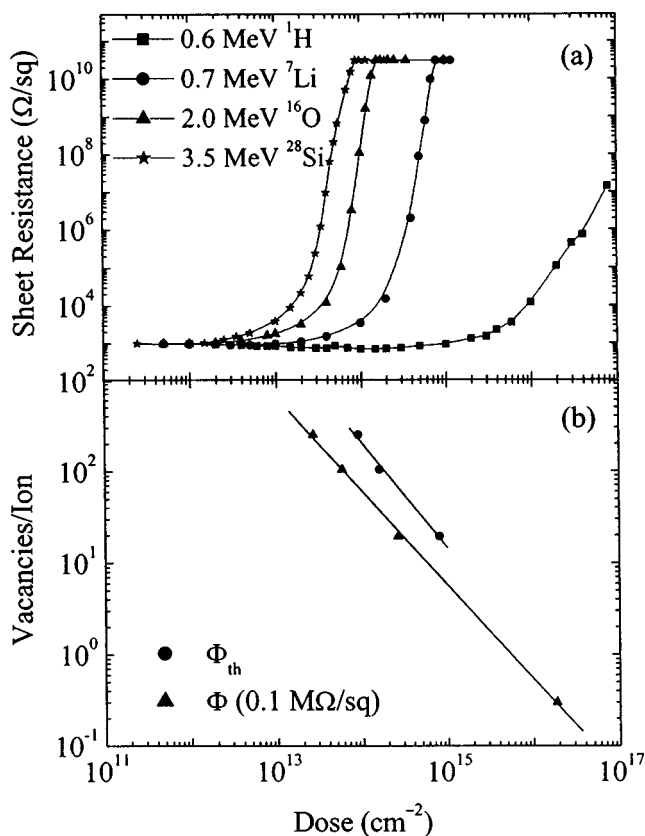


FIG. 1. (a) Dose dependence of sheet resistance of ZnO epilayers bombarded with different ions as indicated (see Table I for the details of implant conditions); (b) average number of ion-beam-generated lattice vacancies within the 0.6- μm -thick ZnO epilayer is plotted vs threshold ion doses Φ_{th} and doses $\Phi(0.1 \text{ M}\Omega/\text{sq})$ required to produce a sheet resistance of 0.1 M Ω/sq , as indicated. Also shown in (b) are straight lines with slopes of -1.14 ± 0.10 and -1.02 ± 0.02 which represent the best fits to Φ_{th} and $\Phi(0.1 \text{ M}\Omega/\text{sq})$ dependencies, respectively.

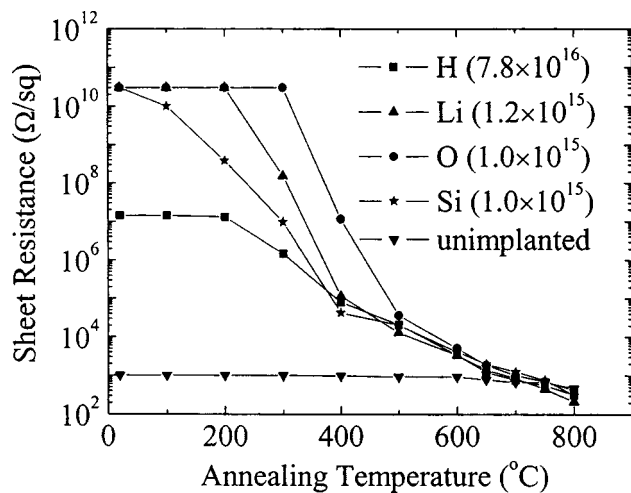


FIG. 2. Evolution of sheet resistance as a function of temperature of isochronal annealing for 60 s of ZnO epilayers bombarded with different ions to different doses (in cm^{-2}), as indicated (see Table I for the details of implant conditions). The evolution of sheet resistance of an as-grown (unirradiated) sample during annealing is also shown for comparison.

small portion of defects survives annihilation and forms stable defect complexes.

Finally, Fig. 2 shows the evolution of R_s as a function of temperature of isochronal annealing of ZnO epilayers bombarded with 0.6 MeV H ions to a dose of $7.8 \times 10^{16} \text{ cm}^{-2}$, 0.7 MeV Li ions to a dose of $1.2 \times 10^{15} \text{ cm}^{-2}$, and 2 MeV O and 3.5 MeV Si ions to a dose of 10^{15} cm^{-2} . Note, that all these doses (except for the case of H ions) are above Φ_{th} , as can be seen from Fig. 1. It is clearly seen from Fig. 2 that, in all the cases studied, defect-induced electrical isolation of ZnO is unstable to RTA at temperatures above $\sim 300^\circ\text{C}$. Figure 2 also shows that, in all cases studied, R_s is recovered to its original value after annealing at $\sim 650^\circ\text{C}$. For comparison, in Fig. 2, we also show the annealing behavior of an as-grown (unirradiated) sample, illustrating that RTA at temperatures below $\sim 700^\circ\text{C}$ has a negligible effect on R_s of as-grown samples. It is also seen in Fig. 2 that the thermal stability of electrical isolation is different for different ion species and doses, consistent with previous studies of electrical isolation in other compound semiconductors.¹⁶ However, presently, more work is obviously needed to better un-

derstand the influence of implant parameters on the thermal stability of electrical isolation in ZnO.

In conclusion, we have demonstrated that sheet resistance of ZnO epilayers can be increased by ~ 7 orders of magnitude as a result of irradiation with MeV light ions. Results have shown that the ion doses necessary for electrical isolation inversely depend on the number of lattice displacements produced by the ion beam. However, such defect-induced electrical isolation of ZnO is thermally stable only for temperatures up to $\sim 300^\circ\text{C}$, and R_s can be completely recovered to its original value by annealing at $\sim 650^\circ\text{C}$. Additional studies on possible chemical isolation would be highly desirable in order to improve the thermal stability of electrical isolation in ZnO, essential for high-temperature/high-power electronic devices.

¹See, for example, J. E. Nause, *III-Vs Rev.* **12**, 28 (1999); Y. Chen, D. Bagnall, and T. Yao, *Mater. Sci. Eng., B* **75**, 190 (2000); D. C. Look, *ibid.* **80**, 383 (2001), and references therein.

²See, for example, S. J. Pearton, *Mater. Sci. Rep.* **4**, 313 (1990).

³D. R. Locker and J. M. Meese, *IEEE Trans. Nucl. Sci.* **19**, 237 (1972); J. M. Meese and D. R. Locker, *Solid State Commun.* **11**, 1547 (1972).

⁴B. W. Thomas and D. Walsh, *J. Phys. D* **6**, 612 (1973).

⁵D. C. Look, D. C. Reynolds, J. W. Hemsky, R. L. Jones, and J. R. Sizelove, *Appl. Phys. Lett.* **75**, 811 (1999).

⁶D. C. Look, J. W. Hemsky, and J. R. Sizelove, *Phys. Rev. Lett.* **82**, 2552 (1999).

⁷F. D. Auret, S. A. Goodman, M. Hayes, M. J. Legodi, H. A. van Laarhoven, and D. C. Look, *Appl. Phys. Lett.* **79**, 3074 (2001); *J. Phys.: Condens. Matter* **13**, 8989 (2001).

⁸K. Koike, T. Tanite, S. Sasa, M. Inoue, and M. Yano, *Mater. Res. Soc. Symp. Proc.* **692**, 11.9 (2002).

⁹J. P. Biersack and L. G. Haggmark, *Nucl. Instrum. Methods* **174**, 257 (1980).

¹⁰H. Boudinov, S. O. Kucheyev, J. S. Williams, C. Jagadish, and G. Li, *Appl. Phys. Lett.* **78**, 943 (2001).

¹¹S. O. Kucheyev, H. Boudinov, J. S. Williams, C. Jagadish, and G. Li, *J. Appl. Phys.* **91**, 4117 (2002).

¹²A slight deviation from the inverse dependence in Fig. 1(b) can be due to, for example, experimental errors or a possible effect of ion beam flux, as discussed in detail in Ref. 11 for the case of electrical isolation of GaN.

¹³H. M. Naguib and R. Kelly, *Radiat. Eff.* **25**, 1 (1975).

¹⁴C. W. White, L. A. Boatner, P. S. Sklad, C. J. McHargue, S. J. Pennycook, M. J. Aziz, G. C. Farlow, and J. Rankin, *Mater. Res. Soc. Symp. Proc.* **74**, 357 (1987).

¹⁵E. Sonder, R. A. Zuhr, and R. E. Valiga, *J. Appl. Phys.* **64**, 1140 (1988).

¹⁶See, for example, T. v. Lippen, H. Boudinov, H. H. Tan, and C. Jagadish, *J. Appl. Phys.* **80**, 264 (2002).